Science of the Total Environment 945 (2024) 174060

Contents lists available at ScienceDirect

Science of the Total Environment

journal homepage: www.elsevier.com/locate/scitotenv

Watershed features shape spatial patterns of fish tissue mercury in a boreal river network

David W. French [*,1], Daniel E. Schindler, Sean R. Brennan, Gordon W. Holtgrieve

School of Aquatic and Fishery Sciences, University of Washington, Seattle, WA, United States of America

HIGHLIGHTS

- Spatial patterns of mercury in an indicator fish were quantified in a large free-flowing river in Alaska.
- Watershed geology & slope best predicted fish tissue Hg and emphasized local controls in Hg rather than downstream transport.
- Watershed scale spatial covariates were better predictors of Hg than in situ dissolved organic carbon.
- Watershed characteristics shape contaminant patterns in riverine food webs.

GRAPHICAL ABSTRACT

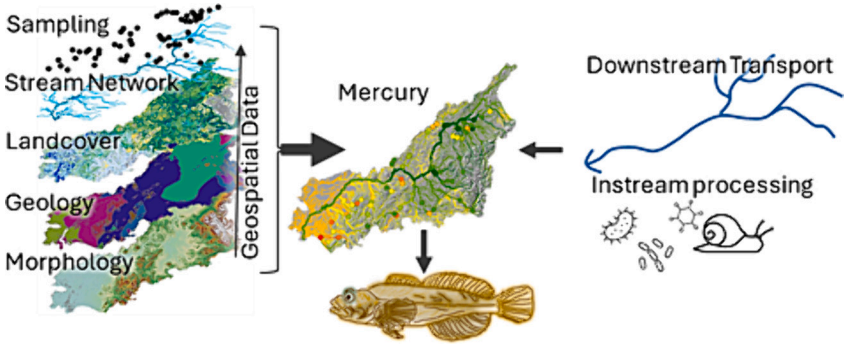

ARTICLE INFO

Editor: Ouyang Wei

Keywords:
Contaminants
Subsistence fisheries
Biogeochemistry
Spatial stream network models

ABSTRACT

Freshwater mercury (Hg) contamination is a widespread environmental concern but how proximate sources and downstream transport shape Hg spatial patterns in riverine food webs is poorly understood. We measured total Hg (THg) in slimy sculpin (*Cottus cognatus*) across the Kuskokwim River, a large boreal river in western Alaska and home to subsistence fishing communities which rely on fish for primary nutrition. We used spatial stream network models (SSNMs) to quantify watershed and instream conditions influencing sculpin THg. Spatial covariates for local watershed geology and slope accounted for 55 % of observed variation in sculpin THg and evidence for downstream transport of Hg in sculpins was weak. Empirical semivariograms indicated these spatial covariates accounted for most spatial autocorrelation in observed THg. Watershed geology and slope explained up to 70 % of sculpin THg variation when SSNMs accounted for instream spatial dependence. Our results provide network-wide predictions for fish tissue THg based largely on publicly available geospatial data and open-source software for SSNMs, and demonstrate how these emerging models can be used to understand contaminant behavior in spatially complex aquatic ecosystems.

* Corresponding author.
E-mail address: davey@naturaldes.com (D.W. French).
[1] Currently at Natural Systems Design, Seattle, WA, United States of America.

https://doi.org/10.1016/j.scitotenv.2024.174060
Received 21 April 2024; Received in revised form 31 May 2024; Accepted 14 June 2024
Available online 20 June 2024

1. Introduction

Mercury (Hg) contamination of aquatic food webs and its potential negative impacts on consumers of fish is a global environmental concern (Krabbenhoft and Rickert, 1995; Selin et al., 2018), but factors governing Hg distributions in river networks remain poorly understood. Hg occurs naturally in nearly all ecosystems, but substantial increases in global environmental Hg concentrations since the mid-19th century are attributed to anthropogenic activity such as fossil fuel combustion, mining, and other industrial processes (Sundseth et al., 2017). Monomethylmercury (MeHg) is the most common toxic form of environmental Hg that bioaccumulates in aquatic ecosystems (Bloom, 1992), and is then biomagnified in food webs that support piscivorous fish (Wiener and Spry, 1996), even in remote waterways with no point sources of Hg (Baker et al., 2009; Southworth et al., 2004). As much as 90 % of MeHg in fish is from dietary uptake (Wiener et al., 2003), and elevated levels of fish tissue MeHg can also reduce reproductive success, damage cells and tissue, and compromise embryonic development in some fish species (Sandheinrich and Wiener, 2011; Wiener and Spry, 1996).

Human exposure to MeHg is primarily via fish and other seafood consumption (Rice et al., 2014; Wiener et al., 2003) and subsistence fishing communities are often vulnerable to high rates of MeHg exposure (Chan and Receveur, 2000; Chan et al., 2003; Oliveira et al., 2010; Trasande et al., 2010) because of their high dependency on both salmon and local freshwater food webs for nutrition. Inorganic Hg in the environment has both local (e.g. watershed geology) and distant (e.g. atmospheric deposition) natural and anthropogenic sources (Sundseth et al., 2017). Net Hg production (e.g., inorganic and organic Hg) is key for Hg to gain entry to food webs, but MeHg production and MeHg bioavailability exhibits substantial spatial variation relative to inorganic Hg (Driscoll et al., 2013; Eagles-Smith et al., 2016). Spatial heterogeneity in Hg within food webs is thus shaped by both local controls on inorganic Hg availability and MeHg production, and transport of these constituents throughout ecosystems. Quantifying how Hg is distributed throughout river networks would provide insight into the processes contributing to spatial variation in inorganic Hg, and management options for controlling exposure to fishery-dependent communities.

Spatial variation in the bioavailability of Hg within aquatic systems is mediated by both watershed and in situ environmental conditions (Driscoll et al., 2013). Regional scale patterning in inorganic Hg is shaped by atmospheric deposition of elemental Hg from anthropogenic emissions and lithospheric reservoirs (e.g., volcanoes) (Fitzgerald et al., 1998); and inorganic Hg loads to inland waters from terrestrial environments generally exceed direct atmospheric inputs to freshwater ecosystems (Hsu-Kim et al., 2018). Watershed characteristics are thus important factors in the delivery of inorganic Hg to the riverine environment. Watershed geology and weathering properties can create subwatershed scale spatial heterogeneity in inorganic Hg, with hydrologic connectivity and landscape characteristics (e.g. flow paths, soil properties) mediating delivery to streams and lakes (Driscoll et al., 2013; Hsu-Kim et al., 2018). At the catchment scale, positive relationships have been shown between inorganic Hg and watershed landcover such as coniferous forest (Drenner et al., 2013) and wetland percentage (Burns et al., 2012; Chasar et al., 2009; Shanley et al., 2012; Wiener et al., 2003), and mining or industrial pollution within a catchment can increase freshwater inorganic Hg concentrations by 1–2 orders of magnitude (Wiener et al., 2003). Broad or regional scale climatic forcing and watershed- or catchment-scale features thus shape inorganic Hg delivery to freshwater systems, but uptake into aquatic food webs throughout river networks exhibits variation at multiple spatial scales (Walters et al., 2010).

Within a river system or water body, spatial patterning in the bioavailability of Hg is largely linked with physical and chemical conditions that promote Hg methylation (Driscoll et al., 2013; Wiener et al., 2003). MeHg formation is positively associated with redox gradients favoring organisms that include sulfate and iron reducing bacteria or methanogens in sediments or the water column (Peng et al., 2024), and high concentrations of organic matter (OM) which fuels microbial metabolism and limits photochemical demethylation of MeHg via light (Klapstein and O'Driscoll, 2018; Wiener et al., 2003). However, recent work shows that specific dissolved OM-associated thiol functional groups dictate MeHg speciation and bioavailability, and that water bodies with very high dissolved OM can limit MeHg bioavailability (Seelen et al., 2023). A global meta-analysis also showed stronger coupling of dissolved organic carbon (DOC) and THg than for MeHg (Lavoie et al., 2019). Recent studies have also shown potential for MeHg formation via aerobic pathways in some aquatic environments, and that a broad range of microorganisms can act as Hg methylators (Rodríguez, 2023).

Channel and valley morphology also play a role in Hg bioavailability. For example, photochemical demethylation of MeHg is positively associated with stream channel size due to increased light availability (Tsui et al., 2013). Previous work has shown positive correlations between fish tissue MeHg and concentrations of sulfate and DOC, and negative correlations with pH, acid neutralizing capacity, and phosphorus concentration (Wiener et al., 2003). Many of these biogeochemical conditions are common attributes of DOC-rich aquatic environments such as wetlands, peat bogs, and lakes, but several studies have found weak or inconsistent relationships between Hg and DOC in rivers (Barbosa et al., 2003; Peterson et al., 2007b). Chasar et al. (2009) however, found a strong positive correlation between fish THg, DOC, and catchment wetlands in 8 different stream types across the U.S. Combined measures of DOC, Hg, and other biogeochemical parameters in tandem with landscape metrics may yield insights into biotic and abiotic factors contributing to elevated Hg in riverine food webs (Hsu-Kim et al., 2018) at the riverscape scale. In particular, there remains a poor understanding of the importance of local habitat conditions that control relevant biogeochemical processes versus downstream transport of Hg from higher in the riverscape.

The Kuskokwim River (Kuskokwim) is a large, free-flowing boreal river in western Alaska that supports over 40 subsistence fishing communities that rely on both anadromous Pacific salmon (*Oncorhynchus* spp.) and resident freshwater fish species for their primary nutrition. Recent catastrophic declines in chum (*Oncorhynchus keta*) and Chinook salmon (*O. tshawytscha*) have led to closures on salmon fisheries which have made freshwater species particularly important for satisfying nutritional needs. The Kuskokwim is the largest river found entirely in Alaska and drains diverse geologic conditions and land cover types. Large swaths of the Kuskokwim watershed coincide with a well-documented metal-bearing mineral deposit that has been actively mined since the early 20th century for Hg, gold, and other metals (Mertie, 1936). Previous work showed elevated levels of THg in fish from heavily mined tributaries in the Kuskokwim (Matz et al., 2017), but this effort was limited in spatial scope to the middle portion of the basin. Additional large-scale mining activity is proposed in remote tributary valleys of the Kuskokwim, including areas where Hg conditions and fish THg have not been studied. Quantifying Hg spatial patterning throughout the Kuskokwim network will aid managers in identifying existing and potential risks to subsistence food resources.

We sampled a ubiquitous small-bodied fish with generalist feeding ecology and a narrow home range (slimy sculpin [*Cottus cognatus*], hereafter 'sculpins') (Gray et al., 2018) throughout the watershed and used recently developed spatial stream network models (SSNMs) (Peterson and Hoef, 2010; Ver Hoef and Peterson, 2010) to identify both watershed scale and in situ biogeochemical factors contributing to THg in resident fish in the Kuskokwim, and to make network-wide predictions of sculpin THg. We expected broad scale spatial patterns in THg driven by source effects from surface geology and watershed morphology and finer scale spatial patterning in THg associated with factors such as wetlands or bogs that shape in situ biogeochemical conditions that influence MeHg availability, such as DOC concentration

and pH. Further, we expected that downstream transport of Hg within the river network would produce characteristic spatial patterning of Hg concentrations in sculpins that would reflect the connection of local food webs to Hg sources further upstream.

2. Methods

2.1. Study area

The Kuskokwim, a large (124,000 km^2) boreal river basin in western Alaska, spans from glacially influenced tributaries in the Alaska range at its eastern margin to the low-lying Yukon-Kuskokwim Delta on the Bering Sea (Fig. 1). The Kuskokwim extends over a complex geomorphologic template overlain by a diversity of land cover types, including barren mountain ranges, forested rolling hills, and broad boreal lowlands and wetland complexes. The eastern and central portions of the Kuskokwim largely coincide with two broad-scale geologic features: the alkaline Farewell terrane comprising complex metamorphosed lithologies of continental origin; and vast Cretaceous flysch deposits of the mineral-bearing Kuskokwim Group (Beikman, 1980; Wilson et al., 2015). The entire Kuskokwim watershed composes a portion of the Tintina Gold Province (TGP), a broad metal-bearing region north of the Denali Fault that spans much of Alaska and the Yukon Territory in western Canada. Previous work in the central Kuskokwim basin found elevated tissue Hg in several fish species harvested by subsistence communities, including dolly varden (*Salvelinus malma*), Northern pike (*Esox lucius*), and burbot (*Lota lota*) (Matz et al., 2017), and historic and active mining activity throughout the TGP has raised broad scale concerns around potential impacts to freshwater resources, fisheries, and subsistence communities.

2.2. Sample collection

Slimy sculpins were collected using a 2 × 6 m stick seine with 7 mm mesh net along river banks at 68 sample sites distributed across the watershed spanning 2nd–8th order streams. Sculpins consume aquatic insects, crustaceans, fish eggs, and small fish. Sculpins are commonly sampled as indicators of environmental conditions due to their small home range and ubiquity in many North American streams (Gray et al., 2018) and they are a species found commonly in the diets of larger predatory species targeted by subsistence fishers. Slimy sculpins were chosen for this study specifically because they have a narrow home range, and thus their tissue chemical composition should reflect local watershed conditions more than fish species that may travel extensively among different watershed areas. Sample sites were chosen to maximize network coverage and to ensure a mixture of sites that share flow (e.g. upstream from one another) and those that do not (e.g. adjacent drainages). A total of 120 sites were sampled for water chemistry, with sculpins collected at 68 sites. A total of 272 sculpins were collected across all sites, with a mean of 5 fish per site; 58 of the 68 sites had 2 or more fish collected, resulting in duplicate or multiple tissue measurements (1 measurement per fish) for the majority (85 %) of sites. Sculpins were euthanized immediately following removal from the stream (IACUC protocol #3142-01), placed in Whirl-Pak bags, and frozen. All samples were stored frozen in the dark until lab processing. At sites with active mining nearby, fish were collected upstream and downstream of observed mining activity, and in the middle of the actively mined reach where accessible. Water samples were collected at all sites where sculpins were collected. The full suite of water chemistry analyses is included in Table S1 and detailed methods on sample analysis are presented in French et al. (2020).

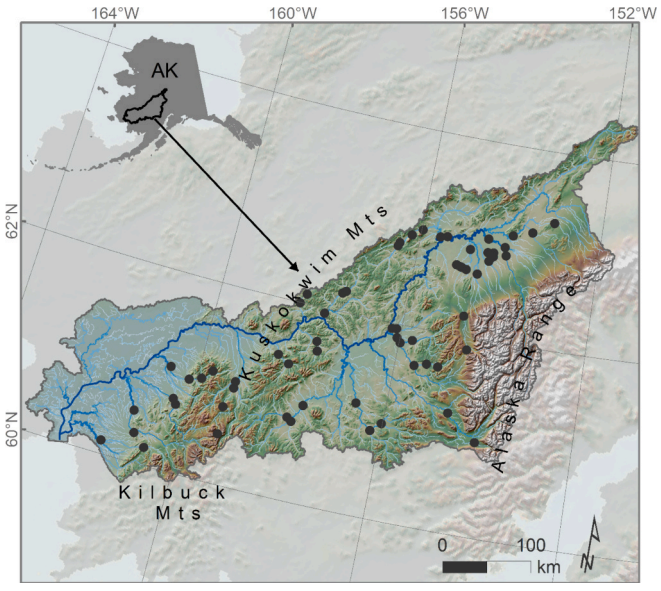

Fig. 1. Map of the Kuskokwim River watershed in Alaska, with shaded relief and stream network and sample sites as black points.

2.3. Mercury analyses

Whole sculpins were weighed, freeze-dried, and then re-weighed in a clean environment at the University of Washington School of Aquatic and Fishery Sciences to measure wet and dry mass. Freeze-dried samples were stored frozen until homogenized and analyzed for THg at the Biotron Analytical Laboratory at Western University in London, Ontario. Samples were analyzed on a Milestone DMA-80 (Milestone Scientific, Inc., Shelton, Connecticut) by thermal decomposition atomic adsorption direct mercury analyzer (DMA) following a modified EPA standard method 7473, lab method TM.0813 (www.standardmethods.org), with a LoD of 0.08 ng and a method reporting limit of 0.24 ng. Mean relative percentage difference in sample duplicates (n = 38) was 2.0 %, with a calibration curve coefficient of determination equal to 0.995. Analysis of a certified reference material (DORM-4) indicated recovery of 97–102 %, with a relative percentage difference of 1 % between duplicate samples (n = 19).

Because inorganic Hg is less bioavailable than MeHg and the majority of THg in fish tissue is present as MeHg, THg is a commonly used surrogate for measuring MeHg concentrations in fish (Driscoll et al., 2013; Wiener et al., 2003). We measured THg from our samples and infer based on previous work in the Kuskokwim by Matz et al. (2017) that 60 % of THg in slimy sculpins in this watershed is MeHg. THg measures from freeze-dried fish were converted to wet mass concentrations using the wet:dry mass ratio for each individual fish. All THg measures provided in this paper are expressed relative to wet fish mass in units of mg kg^{-1}. The correlation between concentrations expressed on a dry mass basis and wet mass basis was 0.99.

2.4. Statistical analysis

We used a statistical modeling approach that includes spatial covariates for watershed features and leverages spatial autocorrelation among sampling sites throughout the Kuskokwim river network based on flow connectivity, flow magnitude, and flow direction (Ver Hoef and Peterson, 2010). We evaluated correlations between THg and a priori candidate covariates and used empirical semivariograms to identify spatial relationships among sample sites. We then fit spatial models (SSNM) for THg using spatial covariates derived for each study site throughout the Kuskokwim. Model performance was assessed to identify both watershed and in situ biogeochemical controls on tissue THg, and variance composition was used to compare the effect size of these controls. Each of these components is detailed below.

2.4.1. Mass-corrections for tissue THg

Positive relationships between fish body size and tissue THg concentrations are well documented for many fish species (Peterson et al., 2007b; Scudder Eikenberry et al., 2015; Walters et al., 2010; Wiener et al., 2003) and a clear positive correlation between THg and fish mass was present in our dataset. As such, we examined mass-corrected fish THg concentrations to understand broader scale watershed and biogeochemical controls on tissue THg versus patterns associated with individual growth. To obtain mass-corrected values, we fit a linear model for $\log_{10}$-transformed tissue THg as a function of $\log_{10}$-transformed fish mass and then used the product of the covariate estimate from that model and each fish's mass to obtain a mass-corrected THg concentration for each sample site. This approach is similar to length-based corrections used in other studies of fish THg (Eagles-Smith and Ackerman, 2014; Eagles-Smith et al., 2016). However, these mass-corrected THg values were then assessed for spatial autocorrelation using empirical semivariance (see below) and mapped to identify spatial patterns in fish THg. Due to spatial autocorrelation in fish mass and to reduce bias in parameter estimation in SSNMs, uncorrected (for mass) fish THg values were used as the response variable and $\log_{10}$-transformed fish mass was included as a covariate in all candidate SSNM models.

2.4.2. Empirical semivariograms

Empirical semivariograms show the strength of spatial dependence between sites at given distances (Olea, 1994), and observed patterns can reveal spatial structure of ecological or biogeochemical processes underlying sample data (McGuire et al., 2014). Semivariogram distances are generally measured as the Euclidean or straight line distance between two sample points (Matheron, 1963); however, hydrologic distance is often a more meaningful spatial dimension for assessing spatial structure in data from stream networks (Cressie et al., 2006; Ganio et al., 2005; Peterson et al., 2006). Hydrologic distance can be further subdivided into flow-connected and flow-unconnected dimensions (Ver Hoef and Peterson, 2010). Flow-connected sites share flow (e.g. a site downstream of another), whereas flow-unconnected sites may share a common downstream junction, but flow does not pass from one site to the other (e.g. adjacent drainages). Fish movement among adjacent tributaries can produce situations where flow-unconnected spatial relationships are important (Isaak et al., 2010). Comparing semivariance in both Euclidian and hydrologic spatial dimensions can yield insights into both watershed and instream factors influencing observations (McGuire et al., 2014).

We calculated semivariance of sculpin THg values according to Euclidean and hydrologic distances using:

$$\gamma(h) = \frac{1}{2|N(h)|} \sum_{N(h)} \left(z_i - z_j\right)^2 \quad (1)$$

where γ is semivariance, N(h) is the set of all pairwise distances i – j = h, |N(h)| is the number of distinct pairs in N(h), and z_i and z_j are data values at spatial locations i and j, respectively (Matheron, 1963). We used a maximum separation distance of 1200 km, 20 lag bins, and a minimum of 15 point pairs per lag bin in semivariance computations. We assessed general trends in spatial dependence, range (distance of asymptote or peak in semivariance), nugget (variance at finest spatial scale), and nested spatial structures as denoted by inflection points in the data (McGuire et al., 2014; Rossi et al., 1992). This approach aids in interpreting spatial scales underlying observed Hg patterns and in covariate and model selection.

2.4.3. Spatial stream network models

We used SSNMs to analyze sculpin THg for all sites sampled (n = 68). These models are described in detail elsewhere (Peterson and Hoef, 2010; Ver Hoef et al., 2006; Ver Hoef and Peterson, 2010) and additional detail is in the supporting information (SI). In brief, these models explicitly account for spatial relationships within a stream network, including flow magnitude, direction, and connectivity. SSNMs provide flexible covariance structures and improve model performance for spatially autocorrelated data (Peterson et al., 2006; Peterson et al., 2007a). Covariance is determined via both hydrologic (tail-up, i.e. flow-connected) and Euclidean distance. We used a mixed-effects modeling framework in which the observed variance in THg across the river network is explained by a set of covariates modeled as fixed effects (e.g., wetland cover %, watershed slope), and these spatial covariance matrices as random effects. All SSNMs were fit within R using the SSN package (R Core Team, 2020; Ver Hoef et al., 2014).

2.4.4. Spatial covariates

Potential covariates were compiled using the STARS toolbox in ArcGIS and publicly available geospatial datasets (Table S2) (Peterson and Hoef, 2014). Watershed covariates for each sample site were accumulated based on upstream drainage areas, and were derived as % cover for categorical datatypes (e.g., wetland cover percent) and as watershed mean values for continuous data (e.g., watershed slope, (French et al., 2020)). All covariates were centered to a mean of 0 and standard deviation of 1 to compare the effect size of covariates. Multicollinearity of spatial covariates was assessed using variance inflation factors. Cross-correlation of covariates was also assessed using Pearson correlation and highly correlated predictors were not used together in candidate models. A set of a priori candidate models was developed and spatial covariates were selected based on factors which we hypothesized to affect instream Hg.

Sample site DOC measures were included in candidate models because DOC and inorganic Hg can be strongly positively correlated in freshwater systems (Lavoie et al., 2019). Sulfate, pH, and alkalinity were also evaluated in candidate models. Mean annual precipitation, watershed slope, and watershed relief were included in candidate models as these factors are expected to affect the movement of water and materials from uplands to the stream channel (Lintern et al., 2018; Smits et al., 2017) and can also influence groundwater transport through bog and peat environments contributing to elevated instream THg (Krabbenhoft and Babiarz, 1992; Krabbenhoft et al., 1995). Watershed wetland cover was also included in candidate models due to positive effects on THg in some river systems (Hurley et al., 1995). Hg-bearing quartz vein systems of the Kuskokwim Mineral Belt within the Tintina Gold Province span much of the Kuskokwim watershed, with Hg occurrences noted throughout the central portion of the watershed between the Takotna and Aniak rivers (Gough and Day, 2010; Miller et al., 2007). A priori model covariates for Hg include a subset of surficial geology types associated with these features. Surface geology was simplified into 12 major groups based on lithology type and age from the Global Lithological Map database (Hartmann and Moosdorf, 2012). A complete list of spatial covariates and data sources is in Table S2. Sample site was also included as a random effect for candidate models to evaluate any site-specific effects on THg in sculpins, sculpin growth, and site-specific factors such as present day or legacy mining impacts.

2.4.5. Variance composition

The flexible covariance structures in SSNMs are well-suited for evaluating the relative effects of watershed controls (e.g., wetlands) and instream processing and transport by examining variance composition (Ver Hoef et al., 2014; Ver Hoef and Peterson, 2010). Variance composition for SSNMs is partitioned among the various autocovariance structures (e.g. Euclidian, flow-connected [tail-up]) and the fixed effects or covariates (e.g. wetland %, DOC). Variance composition was determined to compare the relative proportion of variance explained by the random and fixed effects to evaluate broad scale watershed controls, in situ biogeochemical conditions, and downstream transport processes that mediate tissue Hg in the Kuskokwim.

2.4.6. Model selection

SSNM formulations were initially fit to univariate models, with parameters for hypothesized predictor variables estimated using maximum-likelihood. For these model fits, all runs used the same random effect structure with exponential tail-up (flow-connected, see SI) and Euclidean spatial autocovariance components (Ver Hoef et al., 2014). Univariate models were compared using root mean square prediction error (RMSPE) derived from leave-one-out cross-validation (LOOCV) predictions, and a spatial corrected Akaike information criterion (AIC) (Hoeting et al., 2006). This metric is similar to standard AIC but penalizes SSNMs based on the number of parameters used in the spatial autocovariance structure according to:

$$AIC = -2\backslash\ell_{profile} + 2n\,\frac{p+k+1}{n-p-k-2} \quad (3)$$

where ℓ_{profile} is the profile log-likelihood function (Cressie, 1993), n is the sample size, $p-1$ is the number of covariates, and k is the number of autocorrelation parameters.

Additional candidate predictor variables were then combined with the best covariates in a stepwise fashion, and again selected using RMSPE and AIC. We then compared various spatial autocovariance structures on models fit using restricted maximum likelihood estimation. We expected spatial covariates (e.g. wetland %) to capture the Euclidean spatial structure in our data and for instream conditions (e.g. DOC) and downstream transport to influence the flow-connected (tail-up) dimension. As such, we first fit models for THg using only the fixed effects and a flow-connected spatial dimension for the random error structure. We then computed empirical semivariance for the residual error to evaluate any remaining spatial structure in the data. For comparison, we also fit non-spatial linear models.

2.4.7. Network-wide Hg predictions

The best SSNM was used to develop river-wide predictions for tissue THg. Mean observed sculpin mass (1.9 ± 0.13 g [1 SE]) was used for model predictions. Spatial covariates for model predictions were derived for all 2nd–8th order stream segments in the Kuskokwim using the STARS toolbox in ArcGIS (Peterson and Hoef, 2014).

3. Results

Sculpin tissue THg in the Kuskokwim displayed both watershed-scale and finer-scale instream spatial patterning, generally with lower THg concentrations in the eastern portion of the basin and higher concentrations to the west and lower in the river (Fig. 2), though there were some distinct exceptions to this general trend. THg in sculpin tissues ranged from 0.02 to 0.50 mg kg^{-1} (wet mass), with a mean of 0.13 ± 0.01 mg kg^{-1} (1 SD).

Sculpin THg was positively correlated with fish mass and DOC (Fig. 3a, b). THg was also weakly positively correlated with the Kuskokwim Group geologic formation and sporadic permafrost coverage, derived as watershed percentage upstream of each sample site. THg was negatively correlated with the proportion of the watershed overlain by the Farewell Terrane and with glaciers and barren rock. Sculpin Hg was also negatively correlated with mean watershed slope (Fig. 3c, d, e); flatter regions of the river had higher Hg concentrations in sculpins. For fish at sites downstream of historic or actively mined areas (n = 90), sculpin THg was negatively correlated with distance from mined sites (Fig. 3f).

Semivariograms for sculpin THg revealed distinct spatial structuring in both Euclidian and flow-unconnected spatial dimensions, with weak or random spatial structure in the flow-connected spatial dimension (Fig. 4a). Euclidian spatial dependence increased to a range of approximately 600 km, while flow-unconnected spatial dependence had multi-scale controls, exhibited by inflection points in the semivariograms at ranges of 600, 800 and 1100 km.

The best and most parsimonious SSNM for THg included covariates for fish mass ($\log_{10}$) (β = 0.10), watershed % covered by the Farewell Terrane (β = −0.13), watershed % glaciers and barren rock (β = −0.08), and mean watershed slope (β = −0.07). Of the candidate models for THg, those within 2 AIC points of the best model also included covariates for DOC (β = 0.02), the Kuskokwim Group geologic formation (β = 0.07), and mean watershed relief (β = −0.02, Table S3). In general, the effect sizes (i.e. the β values) for models with similar AIC were roughly 50 % lower than those in the best model, except for the Kuskokwim Group geologic formation which had a similar effect size as watershed slope and watershed % glaciers and barren rock.

The best model for sculpin THg was a full spatial model that included tail-up (flow-connected) autocovariance (Table S4); however, semivariograms of residuals from the non-spatial model (using only fish mass, Farewell Terrane, glaciers, and slope) indicated that most (~60 %) of the spatial structure in THg was captured by fixed effects alone (Fig. 4b, d) as there was little spatial autocorrelation remaining in the residuals of the non-spatial model. Residual variance, RMSPE and AIC were considerably lower for the full spatial model (Fig. 4c), and leave-

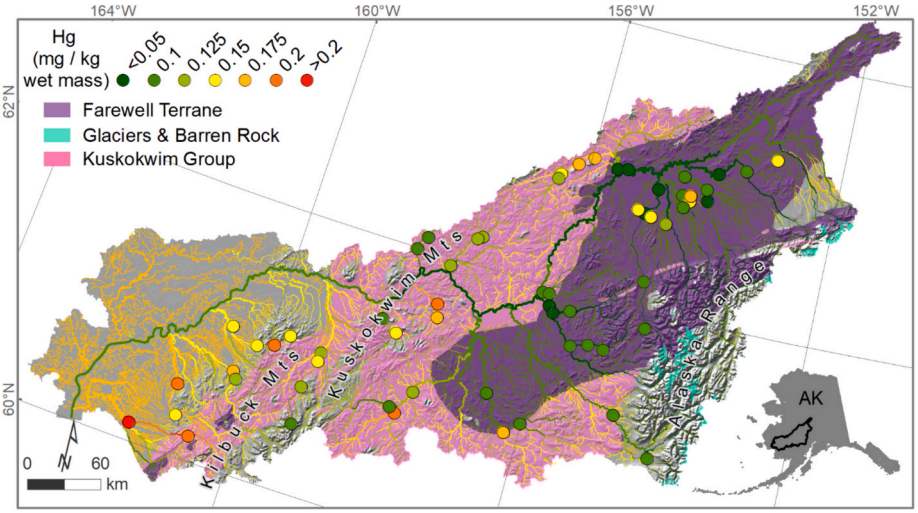

Fig. 2. Map of mass-corrected THg concentrations in sculpins (colored points), network-wide predictions for sculpin tissue THg (colored stream lines), and geologic units used as SSNM spatial covariates for THg. The Kuskokwim Group that contains the Tintina Gold Province is also included for reference, but was not included in the final SSNM for THg.

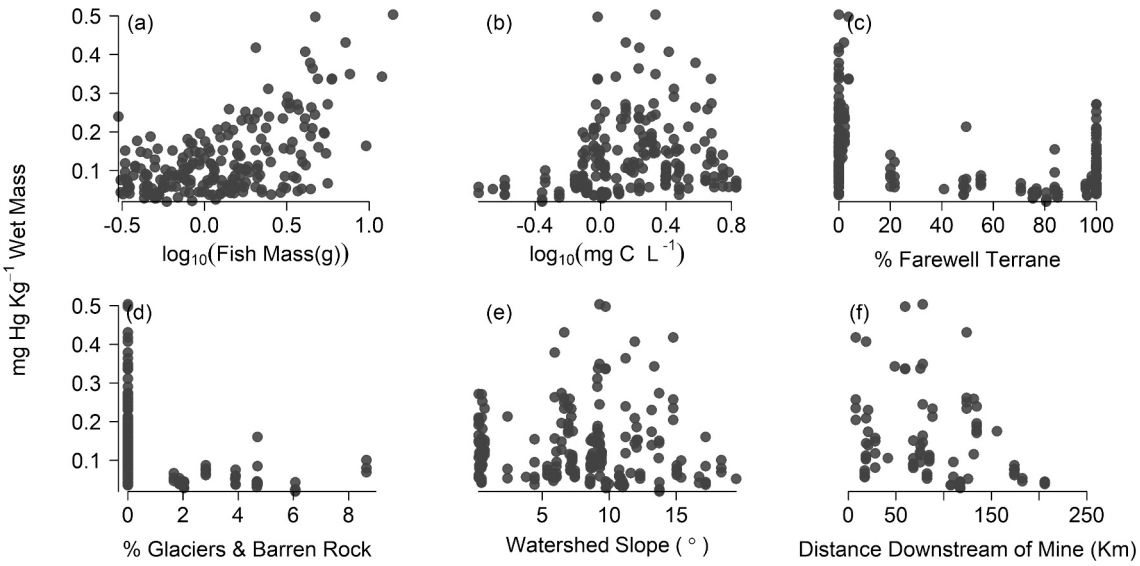

Fig. 3. Scatterplots of sculpin THg versus fish mass (a), dissolved organic carbon concentration (b), watershed cover by the Farewell Terrane geologic unit (c), watershed cover by glaciers and barren rock (d), mean watershed slope (e), and distance downstream of mine sites (f).

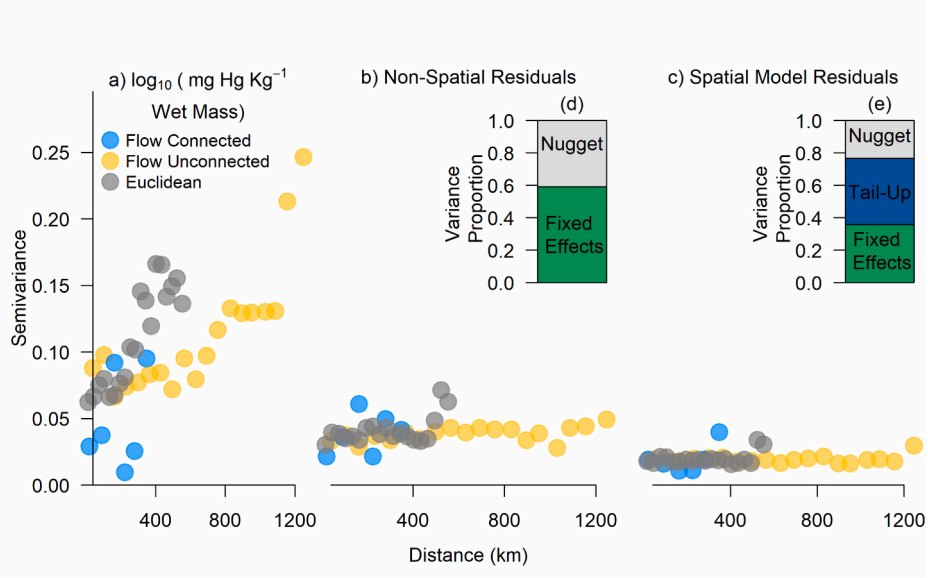

Fig. 4. Empirical semivariograms computed in flow-connected, flow-unconnected, and Euclidian distances for sculpin Hg measurements (a), residuals from a non-spatial model for tissue THg (b), and residuals from a full SSNM model for tissue THg (c). Variance composition for the non-spatial (d) and full SSNM (e) are separated into fixed effects, tail-up (flow-connected) effects, and nugget (random error).

one-out-cross-validation (LOOCV) r^2 was also higher for the full spatial model (Fig. S1). Fixed effects, tail-up, and nugget variance components accounted for 36, 41, and 23 % of the total explained variance in the spatial model (Fig. 4e), though comparison with the non-spatial model suggests that the tail-up component of the spatial model simply captured spatial covariance in the predictors (Fig. 4d).

4. Discussion

Spatial structure in riverine fish THg yields insights into the processes underlying Hg bioavailability to aquatic organisms and their consumers. Spatial patterns for sculpin tissue THg in the Kuskokwim largely reflected broad scale watershed controls, but these watershed controls likely also governed instream biogeochemical conditions mediating Hg bioavailability (French et al., 2020).

The distinct east-west spatial patterning for THg was strongly correlated with broad-scale geologic blocks comprising the alkaline Farewell Terrane and mixed-sedimentary rocks of the Kuskokwim Group (Fig. 1). The Kuskokwim Group in particular includes known metal-bearing quartz veins and has been mined for Hg and other metals for over a century (Goldfarb et al., 2007). These lithologies are also important drivers of instream conditions like alkalinity and pH (Fig. S2, (French et al., 2020)). Previous work in temperate stream systems has shown higher levels of instream THg in lower pH streams, despite uniform atmospheric Hg deposition between study streams (Mason et al., 2000). At low pH free metal ions are more available for transformation and uptake. Low pH can promote complexation of Hg with organic ligands (Watras et al., 1995), including humic acids (Gu et al., 2011), and combined measures of DOC and pH can account for 85–90 % of inorganic Hg variation in lakes (Watras et al., 1995). In the Kuskokwim,

streams draining catchments overlying the Farewell Terrane generally had high pH, high alkalinity, low DOC, and also low THg, whereas those streams draining the Kuskokwim Group and low-lying areas to the west had lower pH, lower alkalinity, higher DOC, and higher THg (Fig. 1, Fig. S2). These broad scale watershed features thus shape biogeochemical conditions affecting Hg bioavailability to sculpins throughout the Kuskokwim watershed.

The effect of DOC on sculpin THg in the Kuskokwim was likely controlled by broad scale geomorphic factors shaping instream biogeochemistry (French et al., 2020). We expected SSNMs for THg to include features associated with DOC-rich environments such as wetlands, bogs, and peat soils. For example, a positive correlation between fish THg and watershed wetland cover was expected due to environmental conditions in wetlands that promote Hg methylation, including an abundance of labile DOC, anaerobic sediments, microbial activity, and seasonal wetting and drying that enhances redox cycles (St. Louis et al., 1994; Wiener et al., 2003). For our dataset; however, broad-scale features like watershed slope and geology were better predictors of sculpin THg than finer scale landscape features such as wetlands and bogs (Table S3). In boreal river systems, low gradient basins generally have lower pH and more colored water (proxy for DOC) (Agren et al., 2014; Varanka et al., 2015). Because both pH and DOC followed similar east-west spatial patterning to THg in the Kuskokwim, the underlying geomorphic mechanisms for this east-west trend (relief, geology) had better predictive power for THg than site-specific DOC. More recent work has shown that specific DOC-associated thiol functional groups mediate MeHg accumulation in aquatic ecosystems (Seelen et al., 2023), and the nature of DOC (e.g., labile vs. recalcitrant) can influence Hg methylation (Ravichandran, 2004). Further characterization of DOC (e.g., the presence of recalcitrant aromatics or functional groups that bind with Hg, Seelen et al., 2023) would help elucidate any relationship between fish THg and DOC in the Kuskokwim. Nevertheless, model results show that a broad scale geomorphic characteristic (i.e., watershed slope) is a watershed feature that exerts strong control on Hg contamination of fishes, probably by controlling the biogeochemical conditions that affect Hg cycling.

The effect of these broad-scale controls is further supported by semivariograms and in variance composition from SSNM models for sculpin THg (Fig. 4b–e). Semivariograms of raw data (Fig. 4a) showed strong spatial dependence in both Euclidian and flow-unconnected space up to broad-scale ranges of 600–1100 km. This spatial range is consistent with the spatial scales of geologic blocks used as spatial covariates in the SSNM models. Flow-unconnected semivariance also exhibited inflection points at roughly 600 and 800 km distances. These distances correspond with major tributary basins within the Kuskokwim that share watershed characteristics such as predominant relief, slope, and geologic blocks which were strongly correlated with sculpin THg. An SSNM with no spatial autocovariance components (Fig. 4b) had little spatial structure remaining in residual semivariance, suggesting that the spatial covariates themselves (Farewell Terrane, watershed slope) accounted for spatial patterning in THg, and that spatial patterning in THg was not strongly controlled by downstream transport along the network. The full spatial model with a tail-up (flow-connected) spatial autocovariance function did reduce overall residual semivariance (Fig. 4c) and improve predictive power (Fig. S1), but the spatial dependence of residuals was similar to the non-spatial model. Inclusion of a tail-down (flow-unconnected) spatial autocovariance function did not improve model performance, likely because sculpins generally do not travel long distances upstream or between flow-unconnected drainages.

Diet is the major pathway of Hg into fish, and we did not assess variation in sculpin diets throughout the Kuskokwim. Our study used sculpin mass as a predictor for THg, which may account for some variation in dietary Hg. Although larger sculpins can consume other small fish, sculpins are obligate generalist benthivores and the majority (85 %) of sculpins' diet is typically on benthic invertebrates (McDonald et al., 1982; Petrosky and Waters, 1975). slimy sculpins are thus at a low trophic level relative to the larger-bodied, piscivorous fish consumed by subsistence communities on the Kuskokwim River. Previous work has shown higher levels of THg in larger, piscivorous fish (e.g. burbot, Northern pike) in Kuskokwim streams draining heavily mined areas in the watershed (Matz et al., 2017). Although our samples included sites adjacent to recently or actively mined areas, we did not sample sites specifically mined for Hg, or 1st order channels sampled by Matz et al. (2017) where THg is elevated. For sites downstream of historically mined areas, sculpin THg did show a positive relationship with proximity to mines (Fig. 2f), however this relationship should be explored further with more accurate and complete current and historic mining data than what is currently publicly available (U.S. Geological Survey, 2008). The pattern observed in our data may simply reflect spatial controls on Hg in streams that happen to coincide with the locations of metal mines in the Kuskokwim watershed.

5. Conclusion

Our results indicate that THg in sculpins from the Kuskokwim reflect both broad scale watershed controls and instream factors. However, the effect of instream conditions on sculpin THg in the Kuskokwim were largely controlled by geomorphic conditions that also control biogeochemistry, such as the effect of watershed slope on DOC in streams (French et al., 2020). Strong Euclidian and flow-unconnected spatial dependence among sample sites also supports the strong effect of broad-scale watershed features on THg when compared to transport processes along the Kuskokwim network. Analysis of the spatial patterning of THg in sculpins demonstrated that sculpins largely reflected local watershed features controlling net Hg (inorganic Hg & MeHg) availability to the food web, and that downstream transport of Hg had minimal effects on Hg in these sedentary species. The use of broad-scale, publicly available geospatial data and SSNMs to predict instream THg in boreal river networks provides an easily accessible approach for resource managers to identify current spatial patterns in Hg contamination and to understand how changing watershed conditions may impact the Hg contamination of subsistence resources in the future under altered climate regimes or changes in land use. This work provides a case study of how emerging SSNMs can be used to understand spatial controls on contaminant production and transport in spatially complex river systems. Furthermore, freshwater fish species are a critical food resource for subsistence communities on the Kuskokwim, when Pacific salmon populations are depressed as they currently are throughout western Alaska. In years with low salmon returns subsistence communities may consume a larger amount of freshwater fish species that are higher in Hg. Understanding the drivers of Hg accumulation in river systems like the Kuskokwim is thus important to managing food resources for these communities.

CRediT authorship contribution statement

David W. French: Writing – review & editing, Writing – original draft, Visualization, Project administration, Methodology, Investigation, Formal analysis, Data curation, Conceptualization. **Daniel E. Schindler:** Writing – review & editing, Writing – original draft, Project administration, Methodology, Investigation, Funding acquisition, Conceptualization. **Sean R. Brennan:** Writing – original draft, Methodology, Investigation, Formal analysis, Data curation, Conceptualization. **Gordon W. Holtgrieve:** Writing – review & editing.

Declaration of competing interest

The authors declare that they have no known competing financial interests or personal relationships that could have appeared to influence the work reported in this paper.

Data availability

Data is available for non-commercial use from the authors. All geospatial data is publicly available, with references in Table S2.

Acknowledgements

We thank J. Baldock and D. Freundlich at the Alaska Salmon Program, Alaska Department of Fish and Game and US Fish and Wildlife Service Yukon Delta National Wildlife Refuge staff, particularly L. Coggins, for assistance with field sampling; A. Shapiro of Alaska Land Exploration, and D. Whited for geospatial data processing. Funding for this research was provided by the Arctic-Yukon-Kuskokwim Sustainable Salmon Initiative and a National Science Foundation Graduate Research Fellowship (#DGE-1762114) to DWF. S.R.B. made substantial contributions to this study and manuscript prior to his passing and is included as an author.

Appendix A. Supplementary data

Supplementary data to this article can be found online at https://doi.org/10.1016/j.scitotenv.2024.174060.

References

Agren, A.M., Buffam, I., Cooper, D.M., Tiwari, T., Evans, C.D., Laudon, H., 2014. Can the heterogeneity in stream dissolved organic carbon be explained by contributing landscape elements? Biogeosciences 11, 1199–1213.
Baker, M.R., Schindler, D.E., Holtgrieve, G.W., St. Louis, V.L., 2009. Bioaccumulation and transport of contaminants: migrating sockeye salmon as vectors of mercury. Environ. Sci. Technol. 43, 8840–8846.
Barbosa, A.C., de Souza, J., Dorea, J.G., Jardim, W.F., Fadini, P.S., 2003. Mercury biomagnification in a tropical black water, Rio Negro, Brazil. Arch. Environ. Contam. Toxicol. 45, 235–246.
Beikman, H.M., 1980. Geologic Map of Alaska. U.S. Geological Survey.
Bloom, N.S., 1992. On the chemical form of mercury in edible fish and marine invertebrate tissue. Can. J. Fish. Aquat. Sci. 49, 1010–1017.
Burns, D.A., Riva-Murray, K., Bradley, P.M., Aiken, G.R., Brigham, M.E., 2012. Landscape controls on total and methyl Hg in the upper Hudson River basin, New York, USA. J. Geophys. Res. Biogeosci. 117.
Chan, H.M., Receveur, O., 2000. Mercury in the traditional diet of indigenous peoples in Canada. Environ. Pollut. 110, 1–2.
Chan, H.M., Scheuhammer, A.M., Ferran, A., Loupelle, C., Holloway, J., Weech, S., 2003. Impacts of mercury on freshwater fish-eating wildlife and humans. Hum. Ecol. Risk. Assess. 9, 867–883.
Chasar, L.C., Scudder, B.C., Stewart, A.R., Bell, A.H., Aiken, G.R., 2009. Mercury cycling in stream ecosystems. 3. Trophic dynamics and methylmercury bioaccumulation. Environ. Sci. Technol. 43, 2733–2739.
Cressie, N.A.C., 1993. Statistics for Spatial Data. Wiley, New York: New York.
Cressie, N., Frey, J., Harch, B., Smith, M., 2006. Spatial prediction on a river network. J. Agric. Biol. Environ. Stat. 11, 127–150.
Drenner, R.W., Chumchal, M.M., Jones, C.M., Lehmann, C.M.B., Gay, D.A., Donato, D.I., 2013. Effects of mercury deposition and coniferous forests on the mercury contamination of fish in the South Central United States. Environ. Sci. Technol. 47, 1274–1279.
Driscoll, C.T., Mason, R.P., Chan, H.M., Jacob, D.J., Pirrone, N., 2013. Mercury as a global pollutant: sources, pathways, and effects. Environ. Sci. Technol. 47, 4967–4983.
Eagles-Smith, C.A., Ackerman, J.T., 2014. Mercury bioaccumulation in estuarine wetland fishes: evaluating habitats and risk to coastal wildlife. Environ. Pollut. 193, 147–155.
Eagles-Smith, C.A., Ackerman, J.T., Willacker, J.J., Tate, M.T., Lutz, M.A., Fleck, J.A., et al., 2016. Spatial and temporal patterns of mercury concentrations in freshwater fish across the Western United States and Canada. Sci. Total Environ. 568, 1171–1184.
Fitzgerald, W.F., Engstrom, D.R., Mason, R.P., Nater, E.A., 1998. The case for atmospheric mercury contamination in remote areas. Environ. Sci. Technol. 32, 1–7.
French, D.W., Schindler, D.E., Brennan, S.R., Whited, D., 2020. Headwater catchments govern biogeochemistry in America's largest free-flowing river network. J. Geophys. Res. Biogeosci. 125, e2020JG005851.
Ganio, L.M., Torgersen, C.E., Gresswell, R.E., 2005. A geostatistical approach for describing spatial pattern in stream networks. Front. Ecol. Environ. 3, 138–144.
Goldfarb, R.J., Marsh, E.E., Hart, C.J.R., Mair, J.L., Miller, M.L., Johnson, C., 2007. Geology and origin of epigenetic lode gold deposits, Tintina Gold Province, Alaska and Yukon: Chapter A in Recent U.S. Geological Survey studies in the Tintina Gold Province, Alaska, United States, and Yukon, Canada—results of a 5-year project. In: Gough, L.P., Day, W.C. (Eds.), Scientific Investigations Report, Reston, VA, p. 22.
Gough, L.P., Day, W.C., 2010. Recent U.S. Geological Survey Studies in the Tintina Gold Province, Alaska, United States, and Yukon, Canada: Results of a 5-Year Project. U.S. Geological Survey, Reston, Va.
Gray, M.A., Curry, R.A., Arciszewski, T.J., Munkittrick, K.R., Brasfield, S.M., 2018. The biology and ecology of slimy sculpin: a recipe for effective environmental monitoring. Facets 3, 103–127.
Gu, B., Bian, Y., Miller, C.L., Dong, W., Jiang, X., Liang, L., 2011. Mercury reduction and complexation by natural organic matter in anoxic environments. Proc. Natl. Acad. Sci. 108, 1479.
Hartmann, J., Moosdorf, N., 2012. The new global lithological map database GLiM: a representation of rock properties at the Earth surface. Geochem. Geophys. Geosyst. 13.
Hoeting, J.A., Davis, R.A., Merton, A.A., Thompson, S.E., 2006. Model selection for geostatistical models. Ecol. Appl. 16, 87–98.
Hsu-Kim, H., Eckley, C.S., Acha, D., Feng, X.B., Gilmour, C.C., Jonsson, S., et al., 2018. Challenges and opportunities for managing aquatic mercury pollution in altered landscapes. Ambio 47, 141–169.
Hurley, J.P., Benoit, J.M., Babiarz, C.L., Shafer, M.M., Andren, A.W., Sullivan, J.R., et al., 1995. Influences of watershed characteristics on mercury levels in Wisconsin Rivers. Environ. Sci. Technol. 29, 1867–1875.
Isaak, D.J., Luce, C.H., Rieman, B.E., Nagel, D.E., Peterson, E.E., Horan, D.L., et al., 2010. Effects of climate change and wildfire on stream temperatures and salmonid thermal habitat in a mountain river network. Ecol. Appl. 20, 1350–1371.
Klapstein, S.J., O'Driscoll, N.J., 2018. Methylmercury biogeochemistry in freshwater ecosystems: a review focusing on DOM and photodemethylation. Bull. Environ. Contam. Toxicol. 100, 14–25.
Krabbenhoft, D.P., Babiarz, C.L., 1992. The role of groundwater transport in aquatic mercury cycling. Water Resour. Res. 28, 3119–3128.
Krabbenhoft, D.P., Rickert, D.A., 1995. Mercury contamination of aquatic ecosystems. In: Fact Sheet, p. 4.
Krabbenhoft, D.P., Benoit, J.M., Babiarz, C.L., Hurley, J.P., Andren, A.W., 1995. Mercury cycling in the Allequash Creek watershed, northern Wisconsin. Water Air Soil Pollut. 80, 425–433.
Lavoie, R.A., Amyot, M., Lapierre, J.F., 2019. Global meta-analysis on the relationship between mercury and dissolved organic carbon in freshwater environments. J. Geophys. Res. Biogeosci. 124, 1508–1523.
Lintern, A., Webb, J.A., Ryu, D., Liu, S., Bende-Michl, U., Waters, D., et al., 2018. Key factors influencing differences in stream water quality across space. Wiley Interdiscip. Rev. Water 5.
Mason, R.P., Laporte, J.M., Andres, S., 2000. Factors controlling the bioaccumulation of mercury, methylmercury, arsenic, selenium, and cadmium by freshwater invertebrates and fish. Arch. Environ. Contam. Toxicol. 38, 283–297.
Matheron, G., 1963. Principles of geostatistics. Econ. Geol. Bull. Soc. Econ. Geol. 58, 1246–1266.
Matz, A., Varner, M., Albert, M., Wuttig, K., 2017. Mercury, Arsenic, and Antimony in Aquatic Biota From the Middle Kuskokwim River Region, Alaska, 2010–2014. Bureau of Land Management.
McDonald, M.E., Cuker, B.E., Mozley, S.C., 1982. Distribution, production, and age structure of slimy sculpin in an Arctic lake. Environ. Biol. Fish 7, 171–176.
McGuire, K.J., Torgersen, C.E., Likens, G.E., Buso, D.C., Lowe, W.H., Bailey, S.W., 2014. Network analysis reveals multiscale controls on streamwater chemistry. Proc. Natl. Acad. Sci. USA 111, 7030–7035.
Mertie, J.B., 1936. Mineral Deposits of the Ruby-Kuskokwim Region Alaska. United States Department of the Interior, Geological Survey: United States Government Printing Office, Washington D.C.
Miller, M.L., Bradley, D.C., Goldfarb, R.J., Bundtzen, T.K., 2007. In: Andrew, C.J., Annesley, I., Archibald, S., Beaudoin, G., Bierlein, F.P., Borg, G., et al. (Eds.), Tectonic setting of Late Cretaceous gold and mercury metallogenesis, Kuskokwim mineral belt, southwestern Alaska, USA. International, pp. 683–686.
Olea, R.A., 1994. Fundamentals of semivariogram estimation, modeling, and usage. In: Yarus, J.M., Chambers, R.L. (Eds.), AAPG Computer Applications in Geology, Tulsa, OK, pp. 27–35.
Oliveira, R.C., Dorea, J.G., Bernardi, J.V.E., Bastos, W.R., Almeida, R., Manzatto, A.G., 2010. Fish consumption by traditional subsistence villagers of the Rio Madeira (Amazon): impact on hair mercury. Ann. Hum. Biol. 37, 629–642.
Peng, X., Yang, Y., Yang, S., Li, L., Song, L., 2024. Recent advance of microbial mercury methylation in the environment. Appl. Microbiol. Biotechnol. 108, 235.
Peterson, E.E., Hoef, J.M.V., 2010. A mixed-model moving-average approach to geostatistical modeling in stream networks. Ecology 91, 644–651.
Peterson, E.E., Hoef, J.M.V., 2014. STARS: an ArcGIS toolset used to calculate the spatial information needed to fit spatial statistical models to stream network data. J. Stat. Softw. 56, 1–17.
Peterson, E.E., Merton, A.A., Theobald, D.M., Urquhart, N.S., 2006. Patterns of spatial autocorrelation in stream water chemistry. Environ. Monit. Assess. 121, 571–596.
Peterson, E.E., Theobald, D.M., Hoef, J.M.V., 2007a. Geostatistical modelling on stream networks: developing valid covariance matrices based on hydrologic distance and stream flow. Freshw. Biol. 52, 267–279.
Peterson, S.A., Van Sickle, J., Herlihy, A.T., Hughes, R.M., 2007b. Mercury concentration in fish from streams and rivers throughout the Western United States. Environ. Sci. Technol. 41, 58–65.
Petrosky, C.E., Waters, T.F., 1975. Annual production by the slimy sculpin population in a small Minnesota trout stream. Trans. Am. Fish. Soc. 104, 237–244.
R Core Team, 2020. R: A Language and Environmental for Statistical Computing. R Foundation for Statistical Computing, Vienna, Austria.
Ravichandran, M., 2004. Interactions between mercury and dissolved organic matter—a review. Chemosphere 55, 319–331.

Rice, K.M., Walker Jr., E.M., Wu, M., Gillette, C., Blough, E.R., 2014. Environmental mercury and its toxic effects. J. Prev. Med. Public Health 47, 74–83.
Rodríguez, J., 2023. Mercury methylation in boreal aquatic ecosystems under oxic conditions and climate change: a review. Front. Mar. Sci. 10.
Rossi, R.E., Mulla, D.J., Journel, A.G., Franz, E.H., 1992. Geostatistical tools for modeling and interpreting ecological spatial dependence. Ecol. Monogr. 62, 277–314.
Sandheinrich, M., Wiener, J., 2011. Methylmercury in freshwater fish: recent advances in assessing toxicity of environmentally relevant exposures. In: Beyer, W., Meador, J. (Eds.), Environmental Contaminants in Biota: Interpreting Tissue Concentrations. CRC Press, Boca Raton, FL, USA, pp. 169–190.
Scudder Eikenberry, B.C., Riva-Murray, K., Knightes, C.D., Journey, C.A., Chasar, L.C., Brigham, M.E., et al., 2015. Optimizing fish sampling for fish–mercury bioaccumulation factors. Chemosphere 135, 467–473.
Seelen, E., Liem-Nguyen, V., Wünsch, U., Baumann, Z., Mason, R., Skyllberg, U., et al., 2023. Dissolved organic matter thiol concentrations determine methylmercury bioavailability across the terrestrial-marine aquatic continuum. Nat. Commun. 14, 6728.
Selin, H., Keane, S.E., Wang, S.X., Selin, N.E., Davis, K., Bally, D., 2018. Linking science and policy to support the implementation of the Minamata Convention on Mercury. Ambio 47, 198–215.
Shanley, J.B., Moore, R., Smith, R.A., Miller, E.K., Simcox, A., Kamman, N., et al., 2012. MERGANSER: an empirical model to predict fish and loon mercury in New England Lakes. Environ. Sci. Technol. 46, 4641–4648.
Smits, A.P., Schindler, D.E., Holtgrieve, G.W., Jankowski, K.J., French, D.W., 2017. Watershed geomorphology interacts with precipitation to influence the magnitude and source of CO_2 emissions from Alaskan streams. J. Geophys. Res. Biogeosci. 122, 1903–1921.
Southworth, G.R., Peterson, M.J., Bogle, M.A., 2004. Bioaccumulation factors for mercury in stream fish. Environ. Pract. 6, 135–143.
St. Louis, V.L., Rudd, J.W.M., Kelly, C.A., Beaty, K.G., Bloom, N.S., Flett, R.J., 1994. Importance of wetlands as sources of methyl mercury to boreal forest ecosystems. Can. J. Fish. Aquat. Sci. 51, 1065–1076.
Sundseth, K., Pacyna, J.M., Pacyna, E.G., Pirrone, N., Thorne, R.J., 2017. Global sources and pathways of mercury in the context of human health. Int. J. Environ. Res. Public Health 14.
Trasande, L., Cortes, J.E., Landrigan, P.J., Abercrombie, M.I., Bopp, R.F., Cifuentes, E., 2010. Methylmercury exposure in a subsistence fishing community in Lake Chapala, Mexico: an ecological approach. Environ. Health 9.
Tsui, M.T.K., Blum, J.D., Finlay, J.C., Balogh, S.J., Kwon, S.Y., Nollet, Y.H., 2013. Photodegradation of methylmercury in stream ecosystems. Limnol. Oceanogr. 58, 13–22.
Alaska Resource Data File (ARDF). In: U.S. Geological Survey, U.S. Geological Survey (Eds.), 2008. U.S. Geological Survey Open-File Report.
Varanka, S., Hjort, J., Luoto, M., 2015. Geomorphological factors predict water quality in boreal rivers. Earth Surf. Process. Landf. 40, 1989–1999.
Ver Hoef, J.M., Peterson, E.E., 2010. A moving average approach for spatial statistical models of stream networks. J. Am. Stat. Assoc. 105, 6–18.
Ver Hoef, J.M., Peterson, E., Theobald, D., 2006. Spatial statistical models that use flow and stream distance. Environ. Ecol. Stat. 13, 449–464.
Ver Hoef, J., Peterson, E., Clifford, D., Shah, R., 2014. SSN: an R package for spatial statistical modeling on stream networks. J. Stat. Softw. 1 (3), 2014.
Walters, D.M., Blocksom, K.A., Lazorchak, J.M., Jicha, T., Angradi, T.R., Bolgrien, D.W., 2010. Mercury contamination in fish in midcontinent great rivers of the United States: importance of species traits and environmental factors. Environ. Sci. Technol. 44, 2947–2953.
Watras, C.J., Morrison, K.A., Host, J.S., Bloom, N.S., 1995. Concentration of mercury species in relationship to other site-specific factors in the surface waters of northern Wisconsin lakes. Limnol. Oceanogr. 40, 556–565.
Wiener, J.G., Spry, D.J., 1996. Toxicological significance of mercury in freshwater fish. In: Beyer, W.N., Heinz, G.H., Redmon-Norwood, A.W. (Eds.), Environmental Contaminants in Wildlife: Interpreting Tissue Concentrations. Lewis Publishers, Boca Raton, FL, pp. 297–339.
Wiener, J.G., Krabbenhoft, D.P., Heinz, G.H., Scheuhammer, A.M., 2003. Ecotoxicology of mercury. In: Hoffman, D.J., Rattner, B.A., Burton, G.A., Cairns, J. (Eds.), Handbook of Ecotoxicology. CRC Press, Boca Raton, FL, USA, pp. 409–463.
Wilson, F.H., Hults, C.P., Mull, C.G., Karl, S.M., 2015. Geologic Map of Alaska. Scientific Investigations Map, Reston, VA.